Soil gas monitoring at the Illinois Basin – Decatur Project carbon sequestration site

Hongbo Shao[*], David A.N. Ussiri[1], Christopher G. Patterson, Randall A. Locke II, Hong Wang, Alexander H. Taylor, Hanna F. Cohen[2]

Illinois State Geological Survey, Prairie Research Institute, University of Illinois at Urbana-Champaign, 615 East Peabody, Champaign, IL 61820, United States

ABSTRACT

An extensive monitoring, verification, and accounting (MVA) program was carried out from 2011 to 2016 as part of the Illinois Basin – Decatur Project (IBDP), a large-scale carbon capture and storage (CCS) demonstration project in Decatur, Illinois, USA. As part of the monitoring program, a near-surface monitoring network for soil gas was used to characterize the natural variability of CO_2 and identify anomalies that could be associated with CO_2 leakage in the vadose zone. In the fall of 2011, 21 permanent soil gas sampling nests were installed on-site and three nests were installed off-site as reference locations. Soil gas was collected from three depth intervals (15–30, 47–61, 107–122 cm) at each nest. Fixed gas (CO_2, N_2, O_2, and light hydrocarbon) concentrations, stable carbon isotopic composition ($\delta^{13}C$), and radiocarbon (^{14}C) content of CO_2 in soil gas were monitored during the pre-injection, injection, and post-injection phases from 2011 to 2016. Both CO_2 concentrations and carbon isotopic compositions showed large spatial and temporal variations; however, the relationships among CO_2, N_2, and O_2 concentrations in soil gas indicated that these variations should be attributed to natural processes and not CO_2 leakage. Soil CO_2 concentrations responded to temperature and precipitation variations and increased with increasing soil depth. While ^{14}C cannot be used to determine the occurrence of CO_2 leakage at IBDP site due to the indistinctive signature between injected CO_2 and soil gas CO_2, experiences at IBDP validated that $\delta^{13}C$ can serve as an effective natural tracer at this site. Results from this project have value for future industrial CCS projects that plan to use soil gas monitoring techniques for site characterization and leakage detection.

1. Introduction

Decisive action is needed to reduce the release of anthropogenic carbon dioxide (CO_2) to the atmosphere in order to help mitigate climate change. Numerous researchers have proposed carbon capture and storage (CCS) as an important strategy for mitigating the future adverse effects of massive amounts of CO_2 emissions (Bachu, 2000; Benson et al., 2012; Bruant et al., 2002; Bruckner et al., 2014; IPCC, 2018). Successful CO_2 storage relies on environmental monitoring to: (1) ensure environmental safety, (2) provide stakeholders with information suitable for CO_2 tracking and accounting efforts, and (3) assist in active project management to decrease project risks. Monitoring of CO_2 storage sites requires an array of monitoring instrumentation and techniques that cover the surface, near surface, and deep subsurface (Jenkins et al., 2015).

Soil gas monitoring aims to detect leakage of CO_2 in the soil vadose zone before it is released into the atmosphere. Such monitoring is valuable because the vadose zone is the final interface between subsurface storage and the atmosphere, and it provides a means of determining whether the injected CO_2 has escaped from the storage reservoir, migrated through the overburden, and reached the unsaturated soil horizon. Clearly demonstrating that this leakage and migration scenario has never occurred is one assurance to site operators, landowners, and the public that CCS operations are safe. However, discriminating CO_2 leakage from natural CO_2 variations in the soil vadose zone can be challenging. A large number of dynamic processes occur in soil that generate or consume CO_2, which leads to large variability in gas concentrations in time and space (Beaubien et al., 2013, 2015; Fessenden et al., 2010; Leuning et al., 2008; Schacht and Jenkins, 2014; Schloemer et al., 2013). For example, soil composition, nutrient provision and

---

[*] Corresponding author.
E-mail address: hbshao@illinois.edu (H. Shao).
[1] Current address: Carbon Management and Sequestration Center, School of Environment and Natural Resources, The Ohio State University, Columbus, OH 43210, United States.
[2] Current address: Department of Geosciences, Western Michigan University, Kalamazoo, MI 49008, United States.

supply, and land utilization influence microbial activity and the respiration of shallow root systems and thus cause large spatial variations of CO_2 concentrations in soil profiles. Temporal changes can be induced by diurnal and seasonal cycles, such as soil temperature and humidity, as well as other more episodic natural factors, such as the microbial population, organic matter concentration, and rainfall distribution (Beaubien et al., 2013, 2015; Fang and Moncrieff, 2001; Qi et al., 2002; Schloemer et al., 2013).

Schloemer et al. (2013) suggested that because of these natural variations, baseline measurements for CCS projects should begin at least three years before CO_2 injection. To identify processes that produce and consume vadose zone CO_2, Romanak et al. (2012, 2014) developed a "process-based" geochemical approach to leakage detection based on the relationships among concentrations of major fixed soil gases (CO_2, O_2, N_2, CH_4). They also suggested that by using this geochemical approach, leakage could be detected without background monitoring. However, Beaubien et al. (2015) pointed out that baseline surveys of near-surface gas geochemistry are important for CCS because they can (1) define the range of natural variation attributable to near-surface processes to minimize false positive or negative detections, and (2) identify preexisting gas migration pathways that may represent a risk for gas-permeable faults.

Another strategy for CO_2 leakage detection at CCS sites is the use of geochemical tracers. Isotopic tracers provide important information about the origin of soil gases (CO_2, CH_4, N_2) and the processes that give rise to their formation (Anderson et al., 2017; Flude et al., 2016; Myers et al., 2013; Romanak et al., 2014; Schoell, 1988; Whiticar, 1999). Natural tracers, especially the $\delta^{13}C$ and ^{14}C content of soil gas CO_2, have been used in CCS monitoring programs (Assayag et al., 2009; Beaubien et al., 2013; Flude et al., 2016; Johnson et al., 2009; Kharaka et al., 2006; Leuning et al., 2008; Mayer et al., 2015; Myrttinen et al., 2010; Schacht and Jenkins, 2014). One of the drawbacks of this strategy, however, is that $\delta^{13}C$ values and ^{14}C content of injected CO_2 may overlap with those of pre-injection soil gas CO_2 signatures which limits the application of this method at some CCS sites (Anderson et al., 2017; Flude et al., 2016; Mayer et al., 2015). For example, at the Weyburn enhanced oil recovery (EOR) site, the $\delta^{13}C$ value of injected CO_2 (-21 to $-20‰$) was comparable to that of the typical soil gas CO_2 composition (Beaubien et al., 2013; Romanak et al., 2014). Mayer et al. (2015) suggested a minimum 5‰ (or under more desirable conditions, 10‰) difference in $\delta^{13}C$ values between injected and baseline CO_2 for this tracer approach to be reliable in determining CO_2 movement and potential leakage.

The radioactive isotope of carbon, ^{14}C in soil gas CO_2 has been suggested as a potentially useful tracer for leakage detection in soil gas monitoring applications (Beaubien et al., 2015; Klusman, 2006, 2011; Mayer et al., 2015; Nickerson and Risk, 2013). The measurement of ^{14}C content in CO_2 for a given gas sample can provide a definite indication of whether the CO_2 is "ancient" or "modern", which can be expressed by "percentage of modern carbon" or PMC (Klusman, 2003, 2011; Beaubien et al., 2013). An advantage of using ^{14}C as a tracer is that there is no biogenic and geogenic production of ^{14}C (Klusman, 2011). Except for anthropogenic sources (mainly nuclear weapon testing), ^{14}C is only generated in the upper atmosphere by the interaction of cosmic rays with atmosphere nitrogen ($^{14}N + n \rightarrow ^{14}C + H$). Because of open-air nuclear weapons testing in the mid-twentieth century, ^{14}C concentrations increased above the 100% pMC value in 1950. After radiocarbon produced in the atmosphere is fixed into organic matter, ^{14}C concentrations decrease at established decay rates. With a half-life of 5700 years, ^{14}C in fossil-fuel-derived CO_2 should have very low values (generally considered as zero) of pMC relative to that produced recently via soil respiration processes, which makes ^{14}C a useful tracer for leakage detection at sites where injected CO_2 is derived from the combustion of fossil fuels (Anderson et al., 2017; Klusman, 2011). Nevertheless, the application of ^{14}C in CCS has been very limited (Beaubien et al., 2013; Klusman, 2011). In this work, we report the

results of the soil gas monitoring program at the Illinois Basin – Decatur Project (IBDP) site through the pre-injection, injection, and post-injection phases from 2011 to 2016. The objectives of this paper are to (1) describe our installation and sampling techniques, (2) characterize subsurface soil gas at a large, demonstration-scale, geological CO_2 sequestration site, including fixed gas (CO_2, N_2, O_2, and light hydrocarbon) concentrations, isotopic composition ($\delta^{13}C$ and ^{14}C) of CO_2 in soil gas, and (3) analyze the data based on known soil gas controlling mechanisms in the vadose zone to look for anomalous conditions that would indicate leakage of injected CO_2. Results from this large-scale CCS demonstration project provide valuable insights for future commercial-scale CCS projects throughout the world and for further environmental assessments related to ongoing demonstration projects in Decatur, Illinois.

2. Approach and methods

2.1. Project description

The Midwest Geological Sequestration Consortium (MGSC) established the IBDP at the Archer Daniels Midland Company (ADM) ethanol production facility in Decatur, Illinois, USA (Finley, 2014). The objective of the project was to validate the capacity, injectivity, and containment of the Mt. Simon Sandstone, which represents the primary carbon storage formation in the Illinois Basin and Midwestern region of the United States. The CO_2 injection operations began on November 4, 2011, and were completed successfully on November 26, 2014, with a total injected mass of 999,215 tons of CO_2. The IBDP included an extensive monitoring, verification, and accounting (MVA) program that used different techniques to monitor the IBDP site from the injection reservoir in the deep subsurface, through the subsurface and near surface, at the surface, and in the atmosphere. The MVA program team began collecting pre-injection monitoring data in 2009 and initiated soil gas monitoring of the near-surface environment later in the project, in September 2011. Near-surface and subsurface monitoring were integral to reaching the following MVA and project goals: (1) establishing pre-injection environmental conditions to evaluate the potential impacts of CO_2 injection, (2) demonstrating that project activities were protective of human health and the environment, and (3) quantifying and tracking CO_2 stored in the Mt. Simon Sandstone.

2.2. Site geology

The deep geology of the site has been described in detail elsewhere (Leetaru and McBride, 2009). In summary, the Mt. Simon Sandstone, an extensive saline formation in the Illinois Basin, which attains a maximum thickness of 792 m in east-central Illinois and west-central Indiana, was the primary target for CO_2 sequestration at the IBDP site. The base of the Mt. Simon Sandstone is underlain by Precambrian igneous bedrock. The 152-m-thick Eau Claire Formation directly overlying the Mt. Simon Sandstone provides the primary seal preventing CO_2 migration into shallower formations. The bottom 61 m of the Eau Claire is primarily shale. The Maquoketa Shale Group and New Albany Shale Group, which are also present at shallower depths, act as secondary and tertiary CO_2 seals, respectively.

Most of the IBDP monitoring was done within a 0.65 km^2 area on ADM property near the CO_2 injection well (Fig. 1). Additional monitoring was also done off-site within 1 km to provide additional reference information at areas distant from the CO_2 injection. The area is mostly flat, with the slope of the land surface ranging from 0 to 2%. Soils at both the on-site and off-site locations are dominantly Drummer silty clay loam (fine-silty, mixed, superactive, mesic Typic Argiudolls) and Flanagan silt loam (fine, smectitic, mesic Aquic Argiudolls) with smaller areas of Proctor and Dana silt loam (< 10% of the area). These soils have high silt (> 50%) and clay contents ($\sim$25%), and are formed from glacial till (Soil Survey Staff, 2014). The drainage class ranges
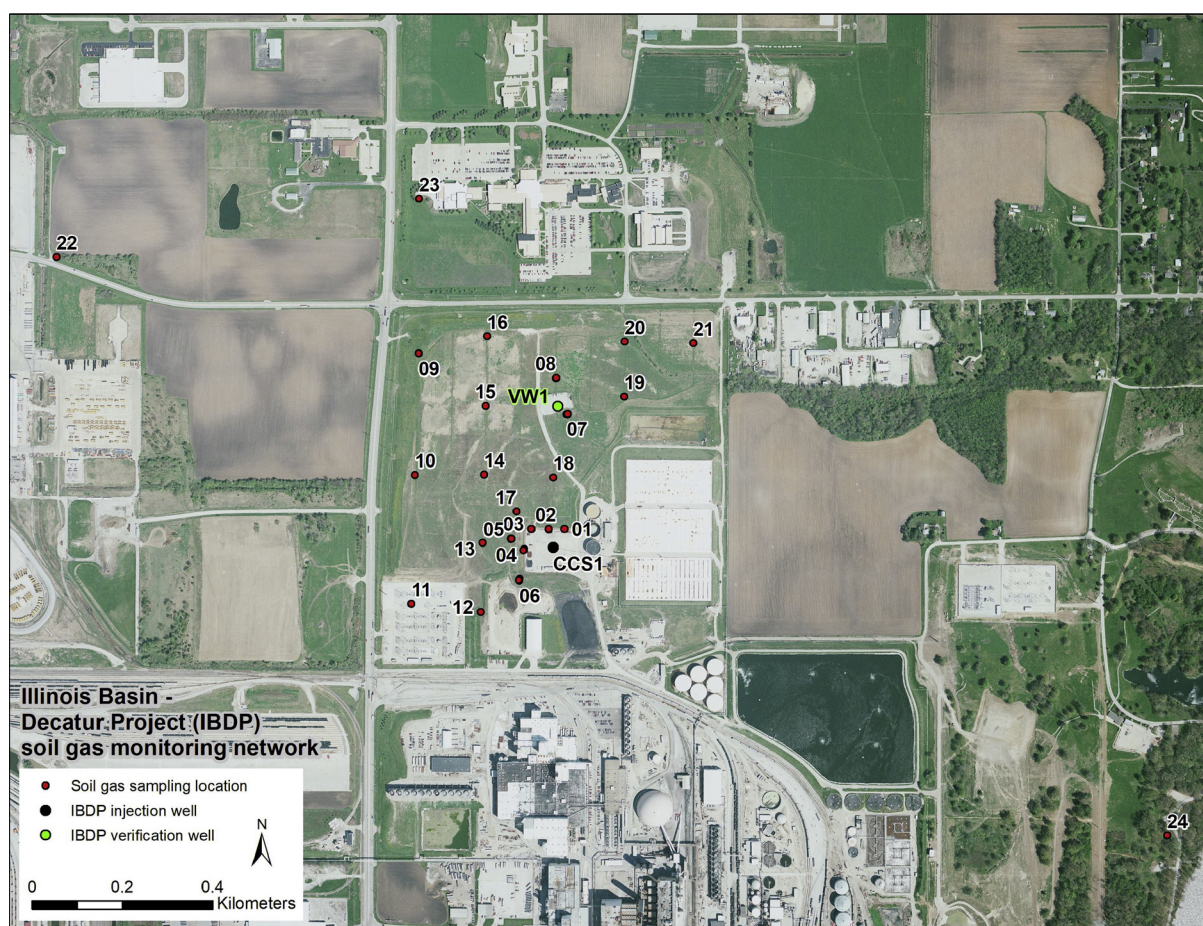
Fig. 1. Map of soil gas network installations at the IBDP site. Numbered locations show soil gas monitoring stations. CCS1 is the IBDP CO_2 injection well. VW1 is the IBDP deep monitoring (verification) well. Aerial photography was acquired on April 30, 2015 by the Illinois Department of Transportation.

from poorly drained to well drained. The water table depth measured at the IBDP site ranged from 0 to 2 m below land surface.

2.3. Weather data

Weather data collected during the monitoring period were obtained from the Decatur Airport weather station, KDEC, (39.83444° − 88.86556°) located about 5 km from the IBDP site. Daily average air temperatures (mean of the maximum and minimum temperatures for each day) from June 2011 through October 2016 (Fig. 2) indicate that temperatures above 20 °C generally occurred at the study site from June to August, whereas temperatures below 0 °C occurred from November through March. The long-term (1981–2000) mean annual precipitation in this area was 976 mm (Table 1). It is worth noting that an extended drought occurred in 2012, with an accumulated annual precipitation (AAP) approximately 200–300 mm less than in other years during the project and 300 mm less than the long-term mean annual precipitation (Knapp et al., 2017). The drought occurred from February to August, followed by greater precipitation (159 mm) in September.

During soil gas monitoring at the IBDP site, soil temperature and moisture were not always measured at each of the 72 individual monitoring points where soil gas was collected. To address the incomplete data set, air temperature and precipitation were used as proxies of soil temperature and soil moisture, respectively. The use of these proxies is appropriate because, first, soil temperature and moisture measured at 10 cm below the soil surface correlated well with the average daily air temperature and monthly precipitation, respectively (unpublished data). Second, previous studies have indicated that
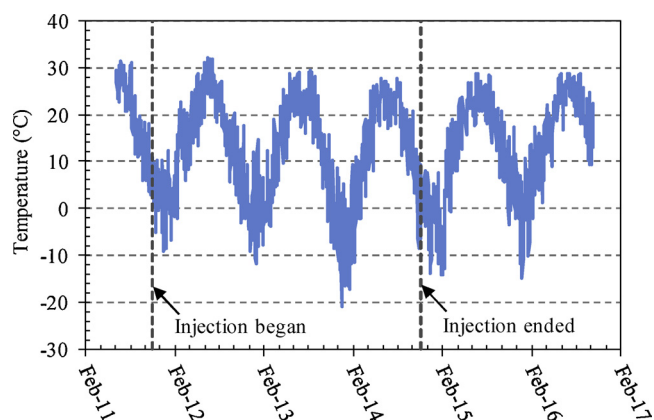

Fig. 2. Daily average air temperature (blue line) at the Decatur Airport (about 5 km from the IBDP site) from 2011 to 2016. The two vertical dashed lines indicate the dates when CO_2 injection began and ended.

soil temperature is closely related to air temperature, and air temperature has often been used to estimate soil temperature (Barman et al., 2017; Gupta et al., 1983; Yener et al., 2017). Third, precipitation is well documented to play an important role in determining soil moisture and microbial activities (Beaubien et al., 2013; He et al., 2012; Xu et al., 2012).

2.4. Soil gas monitoring network installation

The soil gas monitoring network was installed at 21 locations

Table 1
Monthly precipitation (mm) at Decatur Airport, KDEC, from 2011 to 2016.

Year	Jan	Feb	Mar	Apr	May	Jun	Jul	Aug	Sept	Oct	Nov	Dec	AAP[b]
2011	18 (−26)[a]	58 (7)	42 (−26)	159 (62)	141 (32)	189 (78)	15 (−83)	5 (−88)	76 (2)	43 (−40)	106 (18)	58 (−6)	910
2012	51 (7)	32 (−19)	29 (−38)	70 (−27)	43 (−66)	20 (−91)	28 (−70)	68 (−25)	159 (86)	92 (9)	31 (−56)	59 (−5)	682
2013	58 (14)	66 (15)	15 (−52)	169 (72)	166 (57)	133 (23)	80 (−19)	1 (−91)	16 (−58)	103 (19)	28 (−59)	43 (−22)	878
2014	22 (−22)	69 (19)	39 (−28)	114 (17)	65 (−44)	174 (64)	64 (−34)	126 (33)	100 (26)	132 (49)	48 (−39)	52 (−13)	1005
2015	25 (−20)	11 (−39)	43 (−24)	47 (−50)	149 (40)	134 (24)	119 (21)	59 (−34)	55 (−18)	38 (−45)	113 (26)	235 (171)	1028
2016	22 (−22)	15 (−35)	82 (15)	85 (−11)	77 (−32)	55 (−55)	122 (24)	131 (38)	64 (−10)	41 (−42)	92 (5)	24 (−41)	810

[a]Values in parentheses are differences between the total precipitation for that month and year and the long-term average precipitation for that month (negative values indicate less precipitation than the long-term average). Cells shaded in gray indicate that sampling was conducted in that month. The long-term (1981–2010) monthly precipitation averages from January to December were 44, 50, 67, 97, 109, 110, 98, 93, 73, 83, 87, and 65 mm, respectively.
[b]AAP, accumulated annual precipitation. The long-term (1981–2010) mean annual precipitation was 976 mm.

around the project site (Fig. 1). Nests were located more densely near the injection well (CCS1) and the verification well (VW1) because of a general consensus that wells would be the most probable anthropogenic leakage pathways, although leakage could also occur through un-expected pathways away from wells (Carroll et al., 2016). In addition, three off-site locations (soil gas nest SGN-22, SGN-23, and SGN-24), which represent areas farther away from the injection well, were se-lected as reference locations. Twenty-one on-site nests were located in an unused field that had a mix of forbs, graminoids, and infrequent woody shrubs. Off-site nests were located in a grassy area adjacent to a disturbed shrubby area (SGN-22), a lawn (SGN-23), and a wooded area with graminoid ground cover and large trees (SGN-24).

A Geoprobe (Geoprobe Systems, Salina, KS) direct-push drill rig and soil vapor sampling system were used to install sampling screens and collect soil gas samples. The sampling system consisted of a 15-cm-long stainless-steel screen attached to 3.2-mm-diameter polyethylene tubing. The screen was attached to the drive point, and the tubing was inserted through the drive rod of the drill rig. The drive rod was carefully marked to ensure that the exact depth of the screen installation could be determined. The assembly was pushed into the soil to the maximum sampling depth (i.e., 30, 61, and 122 cm) below the surface (Fig. 3A). As the rod was retracted, fine glass beads (60–100 mesh) were poured around the screen to prevent clogging. After the rod was pulled 10 cm above the screen and the screen was completely covered by glass beads, granular bentonite was poured through the drive rod to fill the re-mainder of the probe hole (Fig. 3A). Sample depth, tubing length, and volumes of glass beads and bentonite were carefully measured and re-corded during the installation process. Above the land surface, the polyethylene tubes were tied to steel fence posts near each sampling tube to provide support and protection. After installation, the bentonite was hydrated, and the tubing was capped with a two-way valve to isolate the sampling interval from potential atmospheric air con-tamination through the tubing. For each soil gas nest, three depths were instrumented to provide multilevel soil gas sampling intervals of 15–30, 46–61, and 107–122 cm below the soil surface, hereafter referred to as the shallow, intermediate, and deep intervals, respectively. All nests were purged after the installation, but before the first sampling event, by withdrawing 900 to 1000 mL of soil gas to minimize contamination with atmospheric air and allow equilibration with in situ soil gases. The industrial site host, ADM, permanently removed three nests in August

2013 (SGN-11) and August 2016 (SGN-17 and SGN-18) because of project-related construction.

2.5. Soil gas sampling and analysis

Soil gas from the nests was collected and transferred to pre-evac-uated Cali-5-Bond gas sampling bags (Calibrated Instruments, Inc., McHenry, MD) by using a custom-made assembly consisting of a series of two-way and three-way valves, a vacuum gauge, and two 60-mL disposable syringes attached with Tygon tubing (Fig. 3B). Syringe 1 was used to check for air leaks in the assembly and to evacuate the sampling system. Syringe 2 was used to withdraw the gas sample from the per-manently installed tubing in the soil. The vacuum gauge attached to the assembly was used to monitor the sampling assembly for leakage. Gas samples were collected at 0–5 psi to ensure uniformity in the sampling process and minimize the movement of air into the soil.

Before each sample collection, each gas sampler in a nest was purged by withdrawing and discarding 120 mL of gas (equivalent to approximately two screen and tubing volumes). A preevacuated gas sampling bag was then attached to the gas collection port, followed by further evacuation of the gas sampling bag and sampling unit (10–15 psi). Sixty milliliters of soil gas were then withdrawn and used to condition the gas sampling bag. The bag was again evacuated to prepare for gas collection. For each depth, 600–900 mL of soil gas was withdrawn and directly transferred into a gas sampling bag while avoiding contact between the sampled gas and ambient air to minimize the effects of dilution and contamination.

Samples were transported to the laboratory and analyzed for N_2, O_2, CO_2, and light hydrocarbons (C_1–C_6) with an SRI model 8610 gas chromatograph (GC; SRI Instruments, Torrance, CA). The GC was equipped with an 8600-PK1B 1.8 m × 3.2 mm stainless steel silica gel packed column and an 8600-PK2B 1.8 m × 3.2 mm 5A stainless steel molecular sieve packed column. The GC was equipped with a thermal conductivity detector and flame ionization detector. High-purity helium was used as the carrier gas at a flow rate of 20 cm^3 min^{-1}. The initial oven temperature of 40 °C was increased at 20 °C min^{-1} to 220 °C and maintained at that temperature for 17 min. The GC was calibrated using air and certified low- and high-standard gas mixtures spanning the expected normal concentration ranges. Analyses included numerous replicates, as well as standards and blanks after every 5th to 10th
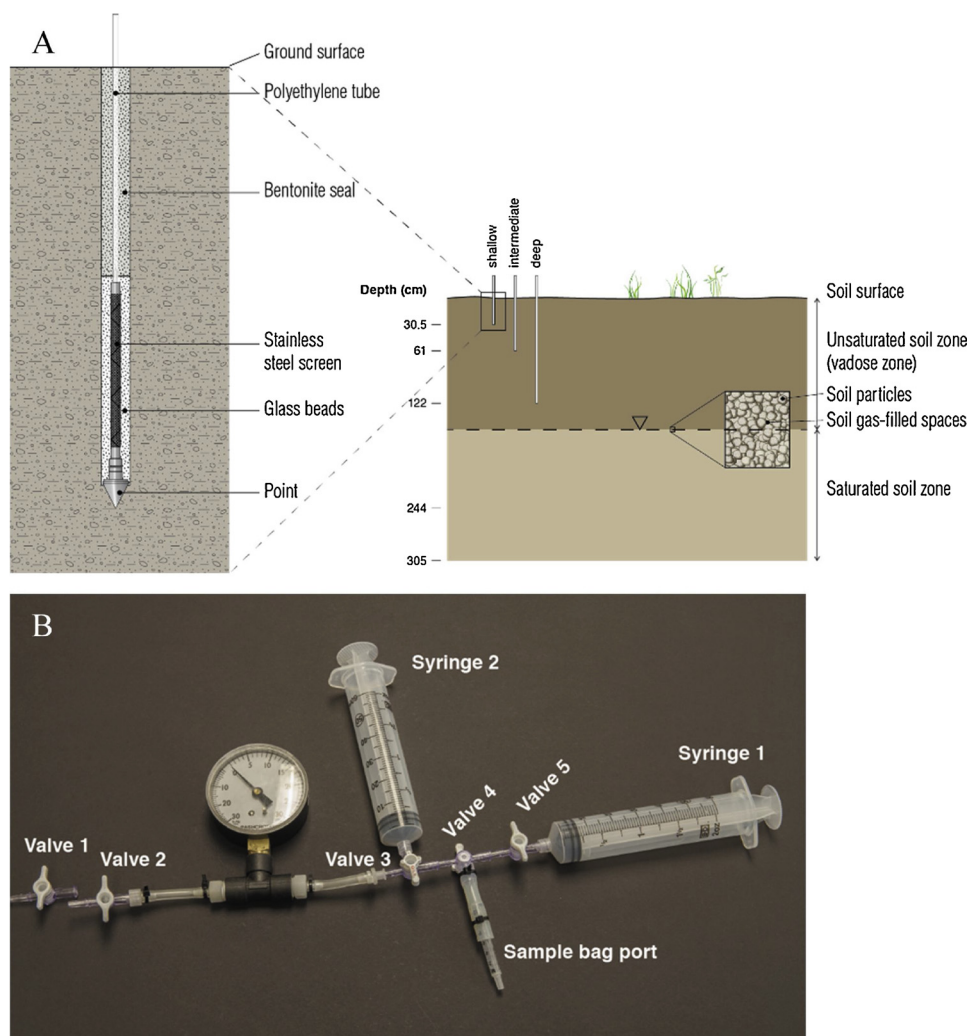
Fig. 3. (A) Schematic diagram of a typical monitoring installation in the soil gas network at the IBDP site, and (B) a photograph of a soil gas sampling device.

sample to verify the precision and accuracy. This chromatographic method does not separate Ar from O_2. To obtain the O_2 concentration, we subtracted the average atmospheric Ar concentration (0.934%) from the concentrations determined by GC analysis (i.e., O_2 + Ar). This treatment is justified by the following reasoning. Because Ar is an inert gas and undergoes almost no chemical reactions or biological processes in soils, Ar concentration in the soil gas is considered the same as its atmospheric concentration when there is no exogenous gas intrusion into the vadose zone (Flude et al., 2016; Hiebert, 1963). In the case of CO_2 leakage from the storage reservoir, the exogenous CO_2 would dilute and thus decrease Ar concentration. Our data correction would result in a maximum 0.934% underestimation of O_2 concentrations in the soil gas which is less than the uncertainty of O_2 measurement (± 2%). In addition, it has been reported that ^{40}Ar and ^{36}Ar are present in deep subsurface reservoirs (Flude et al., 2016; Kipfer et al., 2002). In the leakage scenarios of injected CO_2, deep-derived ^{40}Ar and ^{36}Ar may increase the Ar concentration in the soil gas. However, the typical Ar concentration in the subsurface is generally 1–2 orders of magnitude less than that in the air (Flude et al., 2016). Therefore, our data correction will not significantly change our conclusions. All sample measurements were normalized to 100% for comparison purposes.

In addition to compositional analysis, gas samples from selected nests (SGN-2, SGN-5, SGN-8, SGN-9, SGN-15, SGN-21, SGN-22, SGN-23, and SGN-24) were analyzed for $\delta^{13}C$ values and ^{14}C content. The CO_2 from each soil gas sample was extracted and purified by using a high-vacuum system and was collected cryogenically under less than 5 mTorr

vacuum conditions. The purified CO_2 was split into two aliquots, one for accelerator mass spectroscopy (AMS) ^{14}C analysis and the other for $\delta^{13}C$ analysis. The $\delta^{13}C$ was measured using a dual inlet Finnigan MAT 252 isotope ratio mass spectrometer (Thermo Fisher Scientific, Waltham, MA) at the Illinois State Geological Survey. The ^{14}C content was measured by a hydrogen-iron reduction method at the Keck Carbon Cycle AMS Radiocarbon Dating Laboratory at the University of California, Irvine (Southon, 2007). Background and standard samples were pretreated and analyzed as described previously (Demeter et al., 2012; Stuiver and Polach, 1977; Wang et al., 2009).

3. Results and discussion

3.1. Soil gas composition

Soil gas was collected during: (1) three sampling campaigns before CO_2 injection began (early September 2011, late September 2011, and November 2011), (2) seven campaigns during the injection phase (March 2012, June 2012, September 2012, December 2012, June 2013, September 2013, and June 2014), and (3) two campaigns after injection was completed (October 2015 and September 2016). Off-site locations were not sampled during the first two pre-injection campaigns. Throughout the 6 years of monitoring, soil gas compositional analyses were performed on 755 samples, and 142 samples from selected nests were analyzed for $\delta^{13}C$ values and ^{14}C content. Among the light hydrocarbons (C_1–C_6), only CH_4 and C_3H_8 were occasionally detected and

the concentrations were all less than 0.1% (by volume). Furthermore, fewer than 1% of samples contained light hydrocarbons, and no correlation was found between the presence of hydrocarbons and sampling locations. The measured average dry air composition near the injection well over the monitoring period was 78.1 ± 0.4% N_2, 20.9 ± 0.4% O_2, and 0.07 ± 0.038% CO_2 (the uncertainties are the standard deviation of ten measurements), and the average $\delta^{13}C$ value of atmospheric CO_2 was −8.2 ± 0.8‰ (the uncertainties are the standard deviation of six measurements).

At a CCS site, CO_2 in soil gas can originate mainly from two sources, shallow biologic respiration, and CO_2 leakage from the deep storage reservoir. The former involves in situ consumption of O_2 and production of CO_2 by root respiration (including rhizosphere respiration immediately around the roots) and the decomposition of soil organic matter (SOM) (Amundson et al., 1998; Kuzyakov, 2006). The leakage of CO_2 from deep storage reservoirs through a migration pathway (a fault or leaky well) will add exogenous CO_2 to soil horizons and result in a CO_2 concentration increase in the soil gas and dilution of other pre-existing gasses. Although the range of monitoring parameters caused by biological respiration and deep leakage can overlap, different lines of evidence can be used to distinctly identify the actual origin.

3.1.1. Soil CO_2 concentrations

Natural variations of soil gas CO_2 concentrations at different sampling sites and during different sampling campaigns are expected because both root respiration and SOM decomposition are controlled by soil and meteorological conditions that vary spatially and temporally (Beaubien et al., 2013; Elberling, 2003; Lewicki et al., 2003; Risk et al., 2002; Lewicki et al., 2010). Generally, soil CO_2 concentrations increase with increasing depth in the soil profile and can vary significantly in the near surface soil profile because of soil and meteorological conditions that influence the exchange of soil and atmospheric CO_2 at the soil surface (Lewicki et al., 2003; Risk et al., 2002; Lewicke et al., 2010). In the scenario of CO_2 leakage from a storage reservoir into the vadose zone, soil gas CO_2 concentrations are expected to be greater than baseline concentrations before CO_2 injection, and CO_2 concentrations for on-site locations should be significantly greater than off-site locations (Beaubien et al., 2013; Romanak et al., 2012; Riding and Rochelle, 2009).

At the IBDP site, we observed large temporal and spatial variations of soil gas CO_2 concentrations (Fig. 4). Spatial variations occurred both vertically (at different sampling depth intervals) and horizontally (among sampling nests). In general, CO_2 concentrations increased with increasing sampling depth at a given sample nest. Soil CO_2 concentrations were not statistically different in gas samples collected at on-site

Table 2

Averaged CO_2 concentrations and standard deviations at the intermediate sampling interval for on-site locations at different sampling campaigns.

Project phase	Sampling campaign	Aver. CO_2 (%)	STDEV[a]	CO_2 conc. range[b] (%)
Pre-injection	Sep-2011(a)	0.79	0.62	0.17–1.41
	Sep-2011(b)	0.82	0.62	0.20–1.44
	Nov-2011	0.59	0.34	0.25–0.93
Injection	Mar-2012	1.33	0.74	0.59–2.07
	Jun-2012	0.94	0.68	0.26–1.62
	Sep-2012	1.83	0.60	1.23–2.43
	Dec-2012	1.13	0.57	0.56–1.70
	Jun-2013	3.63	1.76	1.87–5.39
	Sep-2013	0.98	0.79	0.19–1.77
	Jun-2014	2.94	1.88	1.06–4.82
Post-injection	Oct-2015	0.79	0.71	0.08–1.50
	Sep-2016	3.03	1.35	1.68–4.38

[a] STDEV: one standard deviation.
[b] Average CO_2 concentration ± one standard deviation.

locations compared to those collected at off-site locations at the same depth interval and during the same sampling campaign (Fig. 4). The similarity between on-site and off-site soil CO_2 concentrations suggests that spatial and temporal changes in soil CO_2 concentrations at the IBDP site are likely the result of the dynamic nature of in situ biological processes rather than CO_2 leakage from the Mt. Simon Sandstone. However, a comparison of CO_2 concentrations measured between pre-injection and injection/post-injection phases was not conclusive in ruling out CO_2 leakage. For example, while the CO_2 concentrations for samples collected during injection or post-injection phases have no statistical differences with the CO_2 concentrations during the pre-injection phase at the shallow and deep sampling intervals Fig. 4), we found that CO_2 concentrations measured at the intermediate sampling interval for on-site locations during June 2013 and September 2016 campaigns were significantly greater than pre-injection CO_2 concentrations within one standard deviations (Table 2). Thus, we investigated additional soil gas component relationships to evaluate if leakage occurred at the IBDP site.

3.1.2. Relationship between soil gas O_2 and CO_2 concentrations

We applied the geochemical approach of Romanak et al. (2012), which uses either reaction stoichiometry or decoupling of gas components in soil gas to detect the presence of an exogenous CO_2 source. The assumption underlying this approach is that the main production of CO_2 in the vadose zone is from either biological respiration [reaction (1)] or the oxidation of methane [reaction (2)]:
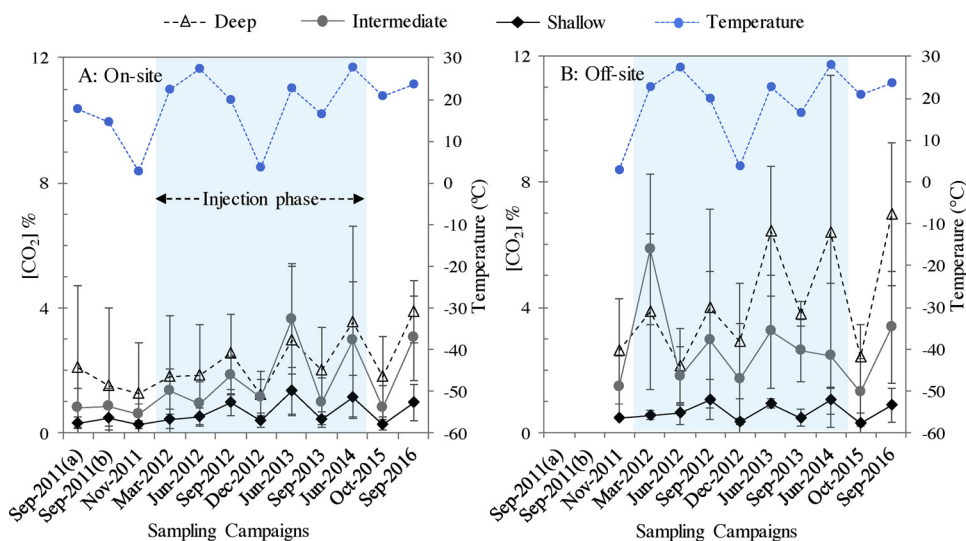

Fig. 4. Averaged CO_2 concentrations in soil gas as a function of time for on-site (A) and off-site (B) locations collected at different depth intervals (shallow; intermediate, and deep). The concentrations were averaged for samples collected from different locations during the same sampling campaign at the same depth intervals. The uncertainties are one standard deviation of the averaged values. The shaded blue area indicates when CO_2 was being injected. The blue dots indicate average air temperatures during the sampling campaigns.
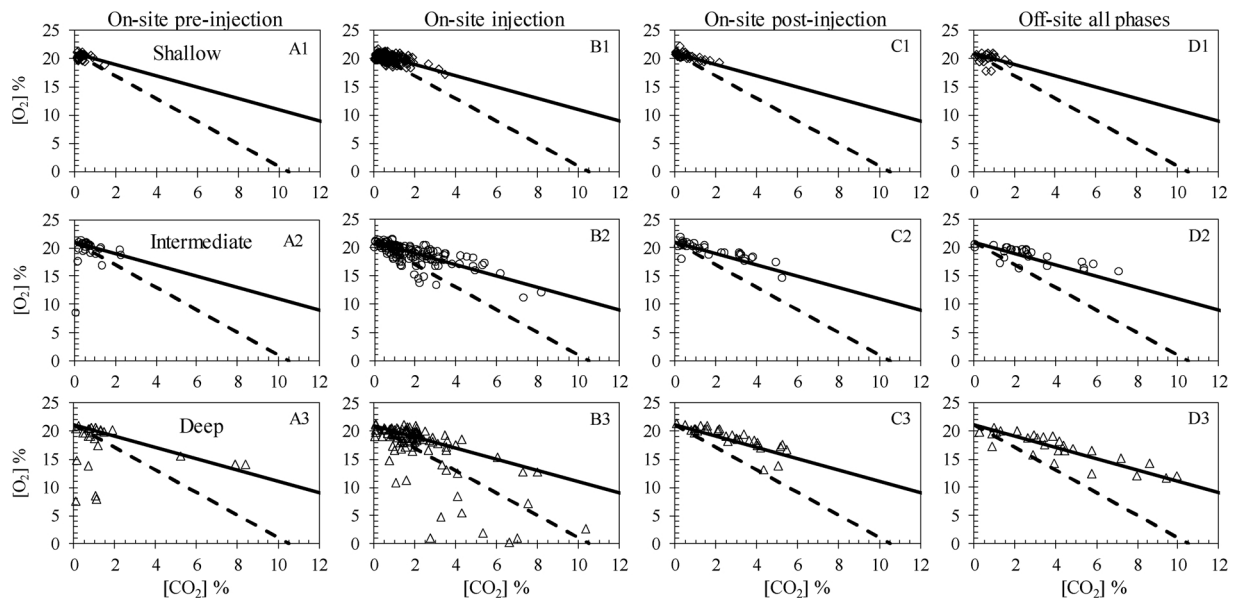
Fig. 5. Relationship between O_2 and CO_2 concentrations in soil gas for on-site (panels A1–A3 for pre-injection; panels B1–B3 for injection; and panels C1–C3 for post-injection) and off-site (panels D1–D3) locations collected at three different depth intervals (shallow, intermediate, and deep). The solid line shows the known trend for natural soil organic carbon oxidation; the dashed line shows the known trend for natural methane oxidation.

$$CH_2O + O_2 = CO_2 + H_2O \qquad (1)$$

$$CH_4 + 2O_2 = CO_2 + 2H_2O \qquad (2)$$

A plot of O_2 versus CO_2 concentration (by volume) should have a slope of -1 for reaction (1) and -2 for reaction (2). A CO_2 concentration greater than what would be expected from a corresponding O_2 concentration in a soil gas sample based on reactions (1) and (2) would suggest an exogenous CO_2 source, indicating a potential leak. A CO_2 concentration smaller than what would be expected from a corresponding O_2 concentration in a soil gas sample based on the oxidation processes outlined above would suggest a CO_2 sink in the soil system, such as dissolution into soil water or reaction with carbonate minerals (Romanak et al., 2012, 2014).

Oxygen versus CO_2 concentrations for IBDP data are plotted in Fig. 5. The solid line shows the idealized soil O_2 to CO_2 relationship based on soil biological respiration processes, and the dashed line shows the idealized relationship for natural methane oxidation. Soil O_2 and CO_2 concentrations at the IBDP site lie either near or below the line representing biological respiration within the analytical error range ($\pm 2\%$ for O_2 and $\pm 0.1\%$ for CO_2) for all three project phases (pre-injection, injection, and post-injection phases) at all three sampling intervals and at both on-site and off-site locations. The observed relationship between soil O_2 and CO_2 at the IBDP site does not support what would be expected for CO_2 leakage scenarios. Therefore, we conclude that the soil CO_2 measured at the IBDP site had a biogenic origin and was not exogenous CO_2. Some soil gas samples collected at the intermediate and deep intervals had CO_2 concentrations that were less than that predicted by the methane oxidation process while some concentrations were between soil biologic respiration and methane oxidation processes. Many soil gas samples with CO_2 concentrations less than that predicted by the methane oxidation line (e.g., Fig. 5A3 and B3), also contained enriched N_2 concentrations compared to atmospheric concentrations, indicating that soil gas CO_2 dissolution or denitrification processes had occurred at these intervals (see further discussion in Section 3.1.3).

3.1.3. Relationship of CO_2 and N_2 concentrations

Nitrogen is generally considered an inert gas. According to reaction (1), under general conditions when methane oxidation [reaction (2)]

and denitrification do not significantly contribute to soil gas composition, the consumption of O_2 and the production of CO_2 from soil biological respiration is a 1:1 ratio (v/v). Thus, N_2 concentrations in soil gas are generally the same as atmospheric N_2 concentrations and are affected only by the addition or removal of other gases that dilute or enrich the N_2 concentration in the soil gas mixture (Beaubien et al., 2013, 2015; Romanak et al., 2012; Schacht and Jenkins, 2014). If CO_2 leakage into the vadose zone had occurred, we would expect decreased soil gas N_2 concentrations in response to the increase of CO_2. CO_2 and N_2 concentration relationships were investigated for soil gas samples collected from both on-site and off-site locations at the IBDP site at the three soil depth intervals during all three operation phases (Fig. 6). The results indicate that the majority of soil gas samples at the IBDP site contained N_2 concentrations similar to air samples collected at IBDP (78.4%) within the analytical error range ($\pm 2.5\%$) (Fig. 6). Nitrogen concentrations in the remaining samples were significantly greater than atmospheric N_2 concentrations. Thus, the N_2 concentrations in the soil gas samples collected from the IBDP site are either similar to or greater than atmospheric N_2 concentrations, which is contrary to the trend expected if leakage of CO_2 had occurred. Data points for samples with exogenous CO_2 are expected to plot in the shaded area with N_2 concentrations smaller than air N_2 concentration (Fig. 6). Therefore, investigation of CO_2 and N_2 relationships for soil gas samples provide another line of evidence that CO_2 leakage from the Mt. Simon Sandstone into the vadose zone did not occur at the IBDP site.

Of the 755 gas samples collected from the IBDP site over the entire monitoring period, 40 samples were found to contain N_2 concentrations in the range of 81–95% (Fig. 6). The significantly greater N_2 concentrations in these samples compared to those in the air suggest N_2 was enriched in these samples. Previous studies have suggested that two natural processes might result in enriched N_2 concentrations in soil gas. One is the dissolution of CO_2 into soil water, and the other is denitrification processes (Romanak et al., 2012; Smith and Arah, 1991). We found that most of the samples with enriched N_2 concentrations were collected in June at the deep or intermediate intervals. Field records also showed that water was drawn into the syringe during soil gas collection for these samples, indicating high soil moisture levels. Because CO_2 is more soluble in water than is N_2 or O_2, CO_2 loss due to dissolution could be expected at the greater depth intervals that had larger soil moisture contents (Riding and Rochelle, 2009). We observed
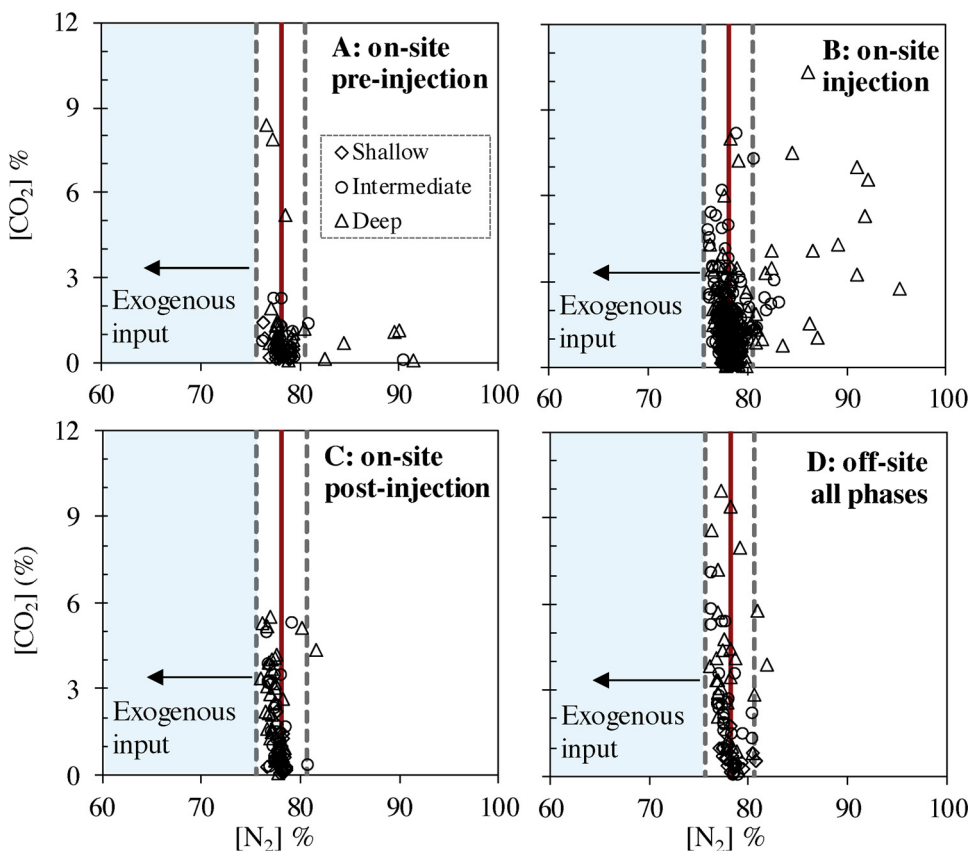
Fig. 6. The relationship between CO_2 and N_2 concentrations in soil gas for on-site (panel A, pre-injection phase; panel B, injection phase; and panel C, post-injection phase) and off-site (D, all phases) locations collected at different depth intervals. The solid red line represents N_2 concentration in the air near at the IBDP site; the two dashed lines show the two boundaries within the analytical error (± 2.5%) for N_2. The shaded area represents where data points with exogenous CO_2 input should locate.

that under soil conditions where the loss of CO_2 from the gas phase could occur via dissolution, a resulting increase in N_2 that exceeded atmospheric concentrations (78.4% at IBDP site) also occurred. Furthermore, up to 67.3 mg/L of nitrate (NO_3^- as N) was detected in shallow groundwater at the IBDP site (unpublished data), suggesting that denitrification processes that convert NO_3^- to N_2 might also have increased soil gas N_2 concentrations at the IBDP site, although documenting denitrification was beyond the scope of the project. Some or all of these potential mechanisms likely occurred at the IBDP site, resulting in larger N_2 concentrations in samples collected in early summer, when the soils were near saturation at the deeper sampling intervals.

Soil gas compositional data suggest that CO_2 leakage from the Mt. Simon Sandstone into the vadose zone did not occur at the IBDP site. Therefore, we attribute the variations of soil gas CO_2 concentrations to in situ geochemical and biological processes. Many parameters, such as soil properties and meteorological conditions, could influence these processes and result in the spatial and temporal variation of soil CO_2 concentrations at the IBDP site as we observed in Fig. 4. For example, the high clay content (~ 25%) in the soil at the IBDP site could result in swelling of clay under wet soil conditions. The swelling process could change gas and water pathways in the soil profile influencing soil CO_2 movement (Ahmed and Abduljauwad, 2018; Zhang et al., 2017). In addition, previous studies have indicated that temperature and rain fall (and thus soil moisture) are two important parameters influencing soil gas CO_2 concentrations, which was reflected from the results of six years of soil gas monitoring at the IBDP site.

We found that even for the sampling campaigns conducted in the same season, CO_2 concentrations could vary widely over different years. For example, five soil gas sampling campaigns were conducted during the fall; early September 2011 [Sep-2011(a), average air temperature of 17.8 °C], late September 2011 [Sep-2011(b), 14.4 °C], September 2012 (20.0 °C), September 2013 (16.4 °C), October 2015 (20.8 °C), and September 2016 (23.6 °C) (Fig. 4). The air temperature

during the September 2016 sampling period was greater than at any other fall sampling event; correspondingly, the average soil CO_2 concentrations at all three sampling depth intervals were greater than in any other fall sampling period (Fig. 4). This observation is consistent with previous reports that soil temperature strongly influences soil CO_2 concentration because of the strong positive exponential correlation between soil temperature and chemical or biological reaction rates (Beaubien et al., 2015; Fang and Moncrieff, 2001; Schloemer et al., 2014). Therefore, soil gas CO_2 concentrations are generally higher in the summer than in other seasons. However, soil gas samples collected in June 2012 contained smaller CO_2 concentrations than in samples collected in September, 2012. The difference in CO_2 concentrations is likely due to differences in moisture conditions between the two campaigns. When soil is dry, root and microbial respiration is generally low, which limits CO_2 production (Liu et al., 2002; Luo and Zhou, 2006). Significant rainfall after a dry season would then create favorable environmental conditions to increase root and soil microbial activity, and increase CO_2 production. Precipitation was significantly reduced during May, June, July, and the first half of August, 2012 (Table 1). After this long dry spell, total precipitation in September 2012 was 159 cm, which was 86 cm higher than the long-term average monthly precipitation in September (Table 1). Therefore, we attribute the smaller CO_2 concentrations in soil gas collected during June 2012 compared to those collected in September 2012 to the 2012 summer drought and the significant precipitation afterward. Other researchers have reported increased soil CO_2 production caused by precipitation events after dry periods, indicating that soil moisture is an important factor influencing CO_2 generation in soil systems (Liu et al., 2002; Luo and Zhou, 2006; Ma et al., 2012; Xu et al., 2004). However, although significant precipitation facilitated CO_2 generation in September 2012, the average CO_2 concentration in this sampling campaign was lower than that in September 2016, when precipitation was insignificant (Table 1) but air temperature was 3.6 °C higher (Fig. 4). This result demonstrated that temperature had a greater impact on CO_2 production than did soil

moisture, although both moisture and temperature are known to play important roles in CO_2 generation and accumulation. This observation is also consistent with previous report by Beaubien et al. (2015).

3.2. Soil gas isotopic characterization

3.2.1. $\delta^{13}C$ of CO_2

As a part of the monitoring program at the IBDP site, the stable isotopic signatures of CO_2 in the soil gas, atmospheric gas, and injected CO_2 were determined. The $\delta^{13}C$ of CO_2 was measured during six soil gas sampling campaigns during the injection and post-injection phases of the project (June 2012, September 2012, June 2013, September 2013, October 2015, and September 2016). For $\delta^{13}C$ of soil CO_2 to be used as a tracer to detect and confirm the absence or presence of CO_2 leakage in the context of CCS, $\delta^{13}C$ data from the pre-injection phase (baseline date) are needed to allow comparison of $\delta^{13}C$ values with the injection/post-injection phases (Schacht and Jenkins, 2014; Flude et al., 2016; Yang et al., 2017). If the $\delta^{13}C$ of a sample collected during injection or post-injection phase is out of the pre-injection phase $\delta^{13}C$ range, it is considered as an anomalous datum, and it may indicate that leakage might have occurred at the site. For the IBDP site, because of the enriched ^{13}C in the injected CO_2 ($\delta^{13}C = -10.7 \pm 0.4$‰), anomalous $\delta^{13}C$ data are expected to be higher than the pre-injection baseline $\delta^{13}C$ (Fig. 7). Unfortunately, due to delayed installation of the network at the IBDP site, pre-injection $\delta^{13}C$ data of soil gas CO_2 were not available. Attempts to use the $\delta^{13}C$ data from samples collected at off-site locations as pre-injection baseline data (the blue shaded area in Fig. 7) identified 18 anomalous $\delta^{13}C$ data points from samples collected at on-site locations during injection and post-injection phases. The anomalous data (in the gray shaded area in Fig. 7) were out of the initially assumed pre-injection baseline $\delta^{13}C$ range (-19.4 to -25.2‰) within the uncertainty of $\delta^{13}C$ measurements (± 0.4‰). This could have been interpreted as that injected CO_2 had leaked from the storage reservoir to these locations, mixed with the natural in situ CO_2, and led to the increased $\delta^{13}C$ of soil gas CO_2. However, based on the relationships of CO_2, O_2, and N_2 concentrations in these samples, we confirmed that there was no exogenous CO_2 in the 13 "anomalous" samples. Thus, the

seemingly anomalous $\delta^{13}C$ values of the 18 samples should actually be attributed to natural variations of $\delta^{13}C$ of soil gas CO_2, and not to CO_2 leakage from the storage reservoir. This discussion highlights that care must be taken when using off-site locations or inadequate pre-injection data to characterize pre-injection conditions. If site conditions are not properly characterized, "false positive" leakage interpretations can be made. These results also highlight the importance of collecting adequate pre-injection data for $\delta^{13}C$ to be used as a tracer for leakage detection (Schloemer et al., 2013).

The $\delta^{13}C$ data collected at the IBDP site indicates that, similar to soil CO_2 concentrations, the $\delta^{13}C$ values of soil CO_2 also varied spatially and temporally. The average $\delta^{13}C$ values of CO_2 in soil gas are plotted as a function of time for both on-site and off-site locations at different depth intervals (Fig. 8). Samples collected during the June 2013 sampling campaign exhibited much lower $\delta^{13}C$ values than did those collected at any other sampling period. Soil gas CO_2 $\delta^{13}C$ values are governed by multiple processes, including CO_2 production by root respiration, oxidation of SOM, fractionation during diffusion when fine-grained sediments are present, isotopic exchange with dissolved inorganic carbon in soil water, or mixing with atmospheric CO_2 (Amundson et al., 1998; Flude et al., 2016; Larson and Breecker, 2014; Mayer et al., 2015). Although all these processes may have contributed to the variations in $\delta^{13}C$ values of soil gas CO_2, mixing with atmospheric CO_2 did not appear to be significant during our sampling campaigns for several reasons. First, CO_2 concentrations in the soil gas samples for isotope analysis were all higher than the atmospheric CO_2 concentration (0.07 ± 0.038%) (Fig. 7). Second, the average $\delta^{13}C$ values at deep and intermediate sampling intervals are not significantly different than that at the shallow sampling interval within one standard deviation (Fig. 8). These results suggest that migration of atmospheric CO_2 into soil gas was not significant even at the shallow sampling depth interval (15–30 cm) which is expected to be more influenced by atmosphere (Lewicki et al., 2003; Risk et al., 2002; Lewicke et al., 2010). Calculations based on simple two end-member mixing model for air and soil gas CO_2 suggests that significant influence of air on $\delta^{13}C$ of soil gas CO_2 only occur when soil gas CO_2 concentrations are close to air CO_2 concentration (Fig. 7). At the IBDP site, soil gas samples for isotopic analysis were all collected during the summer or early fall when root respiration and oxidation of SOM were likely greater than other times of the year and resulted in higher soil CO_2 generation, thus reducing the potential for atmospheric CO_2 to migrate (through advective transport or diffusion) into the soil because of the positive CO_2 concentration gradient between the soil and atmosphere (Kayler et al., 2010; Mayer et al., 2015). In winter, however, the lower soil biotic activity would reduce soil CO_2 concentrations and result in a greater potential for mixing between atmospheric and soil CO_2. This mixing can cause the $\delta^{13}C$ value of soil CO_2 to resemble that of the injected CO_2, producing a potential "false positive" leakage signal. Therefore, isotopic data of soil gas CO_2 collected in the winter when soil gas CO_2 concentrations are low, needs to be interpreted carefully. It is worth noting that the false positive leakage due to mixing of air and soil gas can only occur when the $\delta^{13}C$ value of injected CO_2 is higher than soil gas CO_2. If the $\delta^{13}C$ value of injected CO_2 is lower than that of soil gas CO_2, the increase of $\delta^{13}C$ will not indicate a potential leakage.

If only $\delta^{13}C$ of CO_2 were used to indicate leakage, the lack of on-site, pre-injection data would have made interpretation of the injection and post-injection on-site $\delta^{13}C$ data difficult. However, based on our discussion in Section 3.1, there was no exogenous CO_2 in the soil gas samples collected from the IBDP site during the entire monitoring period. Therefore, a more appropriate $\delta^{13}C$ range of natural soil gas CO_2 from the site should be from -16.0 to -25.6‰ (Fig. 7). This range is 5–15‰ less than the $\delta^{13}C$ values of the injected CO_2 (-10.7 ± 0.4‰), which meets the minimum requirement of a 5‰ difference in $\delta^{13}C$ values as suggested for $\delta^{13}C$ comparisons to be used as a potential indicator of leakage (Mayer et al., 2015). Therefore, based on end-member mixing model for $\delta^{13}C$, it is possible to quantitatively estimate
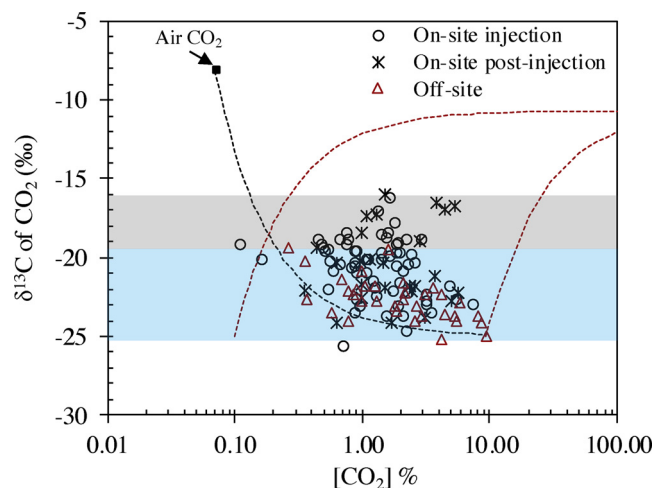

Fig. 7. $\delta^{13}C$ values of soil gas CO_2 as a function of CO_2 concentrations for samples collected from the IBDP site. The blue shaded area represents the $\delta^{13}C$ range at off-site locations (–19.4 to –25.2 ‰). The gray shaded area is the $\delta^{13}C$ range that is out of the off-site location $\delta^{13}C$ range. The dashed black line is a mixing line between air (0.07% and –8.2‰) and soil gas with $\delta^{13}C = -25$‰ at CO_2 concentration range 0.1–9.4%. The two red dashed lines are mixing lines between injected CO_2 ($\delta^{13}C = -10.7$‰) and two soil gas (0.1% and –25‰) and (9.4% and –25‰), respectively. 0.1% and 9.4% are the minimum and maximum CO_2 concentrations detected in samples selected for $\delta^{13}C$ analyses at the IBDP site.
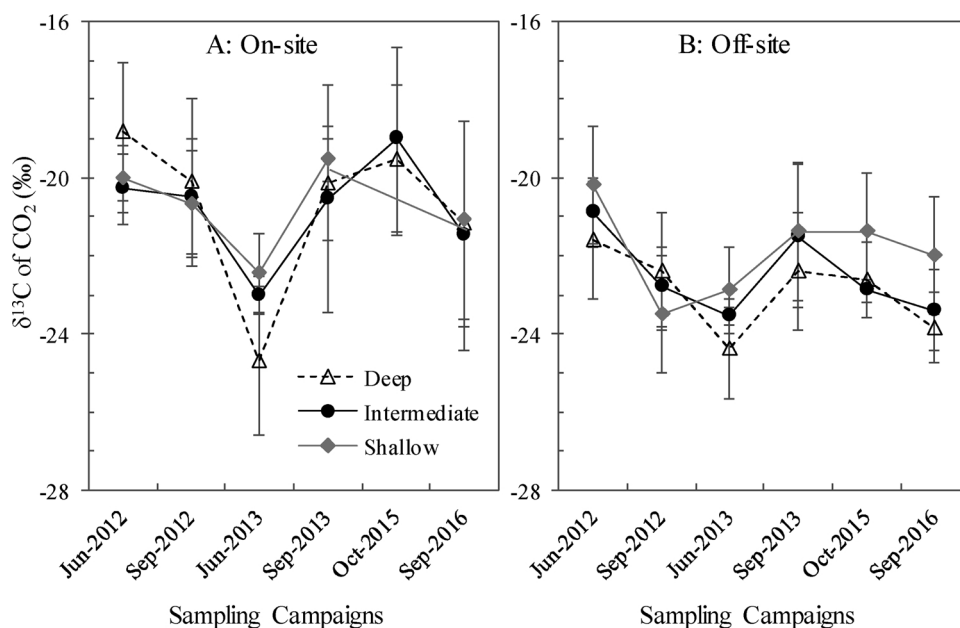
Fig. 8. Average $\delta^{13}C$ values of CO_2 in soil gas during the injection and post-injection phases as a function of time for (A) on-site and (B) off-site locations at different depth intervals. The concentrations were averaged for samples collected from different locations during the same sampling campaign at the same depth intervals. The uncertainties are one standard deviation of the averaged values.

the proportion of injected CO_2 at each sampling location in the scenario of CO_2 leakage (Mayer et al., 2015). Yang et al. (2017) reported the first work to integrate both field tests and numerical modeling to quantitatively assess CO_2 concentration and $\delta^{13}C$ as leakage detection indicators in near-surface environments. They found that $\delta^{13}C$ may have a higher leakage detection probability than CO_2 concentration. However, as the authors pointed out that leakage rate and baseline $\delta^{13}C$ variation are important factors in determining leakage detection probability with $\delta^{13}C$, and the change of $\delta^{13}C$ for the injected CO_2 during the transport from the storage reservoir to the surface will make the estimation more complicated. More research is needed to apply this natural tracer in CCS (Mayer et al., 2015; Flude et al., 2016; Yang et al., 2017).

3.2.2. ^{14}C content of soil CO_2

The pMC of the injected CO_2 at the IBDP site ranged from 100.6 to 108.4% (the two dashed lines in Fig. 9), indicating that the source CO_2 was all modern carbon, consistent with the fact that the source CO_2 was from the fermentation of corn in the production of ethanol. The ^{14}C content of soil gas CO_2 comes from two sources, root respiration and the decomposition of SOM (Amundson et al., 1998; Kuzyakov, 2006). The ^{14}C from root respiration is generally considered to have the similar pMC signature as atmospheric CO_2 (in the range of 97–116%) on the basis that active metabolites in the plants are generated from the present season's photosynthesis, whereas the ^{14}C from decomposition of SOM may have a variable pMC signature that reflects the net contribution of various organic carbon sources that could have different residence times (Amundson et al., 1998; Kuzyakov, 2006; Palstra and Meijer, 2014; Trumbore et al., 1995). The decomposition of plant residue will generate CO_2 with higher pMC values while old humus materials will result in lower pMC of soil gas CO_2 (Beaubien et al., 2013; Kuzyakov, 2006). Values of pMC as low as ~35% were reported for soil gas samples collected at about 1 m below the soil surface (Amundson et al., 1998; Klusman, 2011; Kuzyakov, 2006). Therefore, the pMC of soil gas CO_2 is expected to be in the range of 35–116%. The pMC range of the injected CO_2 at the IBDP site, 100.6–108.4%, thus overlaps with the pMC range of general soil gas CO_2, which makes the use ^{14}C as leakage detection ineffective at this site and others where the source of the injected CO_2 is all modern carbon.

The pMC of soil gas CO_2 at the IBDP site ranged from 87.8 to 107.4% with a majority of these values falling in the atmospheric CO_2 pMC range (97–116%). This result suggests that the CO_2 generated in the soil gas at most locations at the IBDP site was derived through root
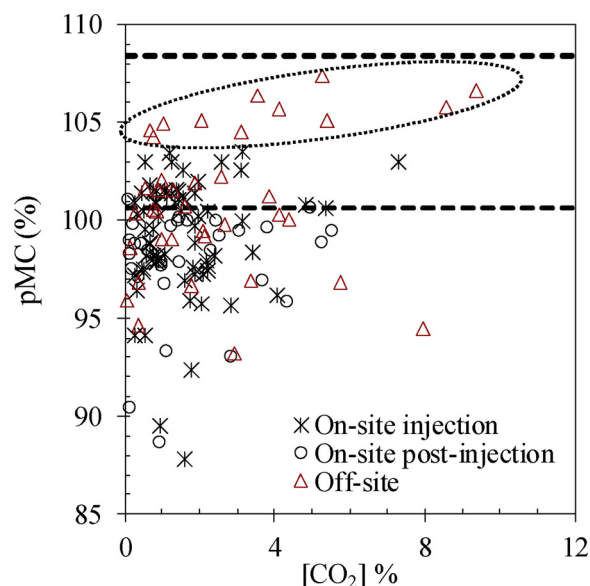

Fig. 9. Soil CO_2 percentage of modern carbon (pMC) distribution as a function of CO_2 concentrations for samples collected from the IBDP site. The dashed lines represent the pMC range of injected CO_2 (100.6–108.4%). The data points inside the oval are for SGN-24.

respiration which has the atmospheric pMC signature, although relatively old carbon was present in soil gas samples collected mostly at the deep sampling interval. For example, the soil gas sample collected from SGN-5 at the deep sampling interval during the June 2012 sampling campaign exhibited the lowest pMC (87.8%) among all the soil gas samples and was dated at approximately 1000 radiocarbon years before present (defined as before 1950). These low pMC values are likely due to microbial processes utilizing SOM that is hundreds to thousands of years old (Amundson et al., 1998; Beaubien et al., 2013). However, during later campaigns, the pMC for this nest at the same depth interval was in the range of 98.9–100.8%, showing that the low pMC value observed in 2012 was not persistent. Among all the nests, only one off-site nest, SGN-24, exhibited persistently high pMC values (104.2–107.4%, points inside the dotted oval in Fig. 9). One plausible explanation for the persistently high pMC is that root respiration from

deep-rooted trees yielded significant contributions to soil CO_2 at SGN-24. Two facts support this hypothesis. First, SGN-24 was the only nest installed in a wooded area with large trees. Second, greater depth intervals showed higher pMC values than did shallow depth intervals, where more biologic activity occurs (Risk et al., 2002).

Both ^{14}C and $\delta^{13}C$ of soil gas CO_2 can serve as natural tracers at different CCS sites. So far, ^{14}C has only been applied for CO_2 leakage detection in a limited number of studies (Anderson et al., 2017; Beaubien et al., 2013; Klusman, 2006, 2011), likely because of the high cost and large sampling volumes required (Beaubien et al., 2015). At the IBDP site, we demonstrated that while ^{14}C cannot be used to determine the occurrence of CO_2 leakage due to the indistinctive signature between injected CO_2 generating from modern carbon sources and soil gas CO_2, $\delta^{13}C$ can serve as an effective natural tracer at this site. However, this conclusion from the IBDP site may not be applicable to other CCS projects. For CCS sites where the injected CO_2 comes from coal-combustion and thus has a similar $\delta^{13}C$ signature as that of near-surface biogenic CO_2, $\delta^{13}C$ cannot serve as an effective tracer for leakage detection (Anderson et al., 2017; Beaubien et al., 2013; Flude et al., 2016; Mayer et al., 2015; Romanak et al., 2014). For these sites, ^{14}C could serve as a good diagnostic indicator for CO_2 leakage, because CO_2 originating from fossil fuel sources has essentially no ^{14}C and near-zero pMC, which is distinctive from the pMC signature of modern soil gas CO_2. In addition, there might be scenarios that both ^{14}C and $\delta^{13}C$ could serve as natural tracers for leakage detection at CCS sites. CO_2 derived from natural gas (old carbon) combustion or gasification may produce CO_2 significantly depleted in ^{13}C with $\delta^{13}C$ well below $-35‰$, thus could be distinctive from the $\delta^{13}C$ signature of soil gas CO_2 (-30 to $-10‰$) (Clark and Fritz, 1997; Mayer et al., 2015; Flude et al., 2016). Therefore, ^{14}C and $\delta^{13}C$ can be effective natural tracers for CCS projects depending on the isotopic signature of the CO_2 used for injection.

4. Conclusions and implications

The IBDP demonstration is one of a few projects in the world that intended to provide learnings for next generation projects by conducting extensive monitoring and assessing the relative value of the various leak detection methods (Jenkins et al., 2012, 2015 and references therein). Six years of soil gas monitoring at the IBDP site has yielded a valuable data set that characterizes the site conditions and exemplifies how soil gas chemistry might be of value in a CCS monitoring context. Large temporal and spatial variations in soil CO_2 concentrations before CO_2 injection into the Mt. Simon Sandstone indicated that dynamic natural processes generated and consumed CO_2. At some sampling locations, greater CO_2 concentrations were observed during the injection and post-injection periods than during the pre-injection period. However, the accumulated monitoring data provided several lines of evidence supporting the conclusion that all the variations in CO_2 concentrations were attributed to natural in situ processes and were not due to CO_2 leakage from the injected CO_2. Comparison of on-site and off-site locations (i.e., control locations) provided the first line of evidence. Soil gas CO_2 concentrations were not statistically different in gas samples collected at on-site locations with those collected at off-site locations at the same depth intervals and during the same sampling campaign.

Evaluating the relationships among fixed gas concentrations in soil gas was another means to verify that CO_2 leakage to the vadose zone did not occur at the IBDP site. Plotting the relationships of O_2 or N_2 concentrations with CO_2 concentrations and comparing them with anticipated relationships provide two lines of evidence and clearly separate signals associated with in situ natural biogenic CO_2 from exogenous CO_2. Results from the IBDP site indicated that the differences in the magnitude and variability of CO_2 concentrations were attributed to natural processes, biologic respiration, and geochemical reactions, and not due to CO_2 leakage from the storage reservoir. Evaluating the

concentration relationships of various components in soil gas can minimize false positives (i.e., natural processes incorrectly interpreted as leakage) or false negatives (leakage signals masked by natural, biogenically mediated variability).

At the IBDP site, due to lack of pre-injection $\delta^{13}C$ data, we were not able to use stable carbon isotope results alone to determine if leakage had occurred at this site. However, our results indicate that the injected CO_2 had a distinct $\delta^{13}C$ signature, compared with the $\delta^{13}C$ range of the soil gas CO_2. Thus, $\delta^{13}C$ could serve as an effective natural tracer for leakage detection at the IBDP site should future CO_2 injection occur. In addition, due to similar ^{14}C signatures of injected CO_2 and soil gas CO_2, ^{14}C could likely not be used to determine the occurrence of CO_2 leakage at the IBDP site. However, for CCS projects using CO_2 from old carbon sources (e.g., from combustion of fossil fuels) that essentially have no ^{14}C and near-zero pMC, ^{14}C would serve as a good diagnostic indicator for CO_2 leakage detection. ^{14}C and $\delta^{13}C$ can be effective natural tracers for CCS projects under different conditions given there is no overlap of carbon isotope signature between injected CO_2 and natural soil gas CO_2.

Although soil gas monitoring is a valuable means of leakage detection for CCS projects, the six years of soil gas monitoring at the IBDP site suggest that this monitoring method requires extensive efforts to install, maintain, and sample the monitoring network. The costs and benefits of using this technique need to be assessed on a case-by-case basis for potential use at future projects. We suggest that if soil gas monitoring is used, soil gas surveys should be conducted on-site and off-site during the pre-injection phase for at least one year to incorporate seasonal and temporal variability of ^{13}C and ^{14}C components of soil gas CO_2. Ideally, pre-injection monitoring data would include a range of observed seasonal patterns over multiple years. Sampling during the injection and post-injection periods should include both on-site locations and carefully selected off-site locations during periods with relatively low soil biological activity. In addition, future projects will need to consider new autonomous techniques for soil gas monitoring presently being developed that could be combined with manual sampling (Beaubien et al., 2015; Jenkins et al., 2015; Klusman, 2011; Mayer et al., 2015; Romanak et al., 2014 and references therein). Overall, soil gas monitoring is useful in conjunction with other monitoring techniques to evaluate anomalous signals, attribute sources of variability, and if needed, define the extent and magnitude of CO_2 leakage should it occur at a CCS storage site.

References

Ahmed, H.R., Abduljauwad, S., 2018. Significance of molecular-level behaviour incorporation in the constitutive models of expansive clays – a review. Geomech. Geoeng. Int. J. 13, 115–138.

Amundson, R., Stern, L., Baisden, T., Wang, Y., 1998. The isotopic composition of soil and soil-respired CO_2. Geoderma 82, 83–114.

Anderson, J.S., Romanak, K.D., Yang, C., Lu, J., Hovorka, S.D., Young, M.H., 2017. Gas source attribution techniques for assessing leakage at geologic CO_2 storage sites: evaluating a CO_2 and CH_4 soil gas anomaly at the Cranfield CO_2-EOR site. Chem. Geol. 454, 93–104.

Assayag, N., Matter, J., Ader, M., Goldberg, D., Agrinier, P., 2009. Water–rock interactions during a CO_2 injection field-test: implications on host rock dissolution and alteration effects. Chem. Geol. 265, 227–235.

Bachu, S., 2000. Sequestration of CO_2 in geological media: criteria and approach for site selection in response to climate change. Energy Convers. Manage. 41, 953–970.

Barman, D., Kundu, D.K., Pal, S., Pal, S., Chakraborty, A.K., Jha, A.K., Mazumdar, S.P., Saha, R., Bhattacharyya, P., 2017. Soil temperature prediction from air temperature for alluvial soils in lower Indo-Gangetic plain. Int. Agrophys. 31, 9–22.

Beaubien, S.E., Jones, D.G., Gal, F., Barkwith, A.K.A.P., Braibant, G., Baubron, J.C., Ciotoli, G., Graziani, S., Lister, T.R., Lombardi, S., Michel, K., Quattrocchi, F., Strutt, M.H., 2013. Monitoring of near-surface gas geochemistry at the Weyburn, Canada, CO_2-EOR site, 2001–2011. Int. J. Greenh. Gas Control 16, S236–S262.

Beaubien, S.E., Ruggiero, L., Annunziatellis, A., Bigi, S., Ciotoli, G., Deiana, P., Graziani, S., Lombardi, S., Tartarello, M.C., 2015. The importance of baseline surveys of near-surface gas geochemistry for ccs monitoring, as shown from onshore case studies in Northern and Southern Europe. Oil Gas Sci. Technol. Rev. d'IFP Energies N. 70, 615–633.

Benson, S.M., Bennaceur, K., Cook, P., Davison, J., de Coninck, H., Farhat, K., Ramirez, A., Simbeck, D., Surles, T., Verma, P., Wright, I., 2012. Carbon capture and storage. In: Johansson, T.B., Nakicenovic, N., Patwardhan, A., Gomez-Echeverri, L. (Eds.), Global Energy Assessment: Toward a Sustainable Future. Cambridge University Press, Cambridge, UK, pp. 993–1068 International Institute for Applied Systems Analysis, Laxenburg, Austria.

Bruant, R.G., Guswa, A.J., Celia, M.A., Peters, C.A., 2002. Safe storage of CO_2 in deep saline aquifers. Environ. Sci. Technol. 36, 240A–245A.

Bruckner, T., Bashmakov, I.A., Mulugetta, Y., Chum, H., Navarro, A.d.l.V., Edmonds, J., Faaij, A., Fungtammasan, B., Garg, A., Hertwich, E., Honnery, D., Infield, D., Kainuma, M., Khennas, S., Kim, S., Nimir, H.B., Riahi, K., Strachan, N., Wiser, R., Zhang, X., 2014. Energy systems. In: Edenhofer, O., Pichs-Madruga, R., Sokona, Y., Farahani, E., Kadner, S., Seyboth, K., Adler, A., Baum, I., Brunner, S., Eickemeier, P., Kriemann, B., Savolainen, J., Schlömer, S., Stechow, C.v., Zwickel, T., Minx, J.C. (Eds.), Climate Change 2014: Mitigation of Climate Change. Contribution of Working Group III to the Fifth Assessment Report of the Intergovernmental Panel on Climate Change. Cambridge University Press, Cambridge, UK, pp. 511–597.

Carroll, S., Carey, J.W., Dzombak, D., Huerta, N.J., Li, L., Richard, T., Um, W., Walsh, S.D.C., Zhang, L.W., 2016. Role of chemistry, mechanics, and transport on well integrity in CO_2 storage environments. Int. J. Greenh. Gas Control 49, 149–160.

Clark, I.D., Fritz, P., 1997. Environmental Isotopes in Hydrogeology. Lewis Publishers, Boca Raton, New York.

Demeter, F., Shackelford, L.L., Bacon, A.M., Duringer, P., Westaway, K., Sayavongkhamdy, T., Braga, J., Sichanthongtip, P., Khamdalavong, P., Ponche, J.-L., Wang, H., Lundstrom, C., Patole-Edoumba, E., Karpoff, A.-M., 2012. Anatomically modern human in Southeast Asia (Laos) by 46 ka. Proc. Natl. Acad. Sci. USA 109, 14375–14380.

Elberling, B., 2003. Seasonal trends of soil CO_2 dynamics in a soil subject to freezing. J. Hydrol. 276, 159–175.

Fang, C., Moncrieff, J.B., 2001. The dependence of soil CO_2 efflux on temperature. Soil Biol. Biochem. 33, 155–165.

Fessenden, J.E., Clegg, S.M., Rahn, T.A., Humphries, S.D., Baldridge, W.S., 2010. Novel MVA tools to track CO_2 seepage, tested at the ZERT controlled release site in Bozeman, MT. Environ. Earth Sci. 60, 325–334.

Finley, R.J., 2014. An overview of the Illinois Basin–Decatur Project. Greenh. Gases: Sci. Technol. 4, 571–579.

Flude, S., Johnson, G., Gilfillan, S.M., Haszeldine, R.S., 2016. Inherent tracers for carbon capture and storage in sedimentary formations: composition and applications. Environ. Sci. Technol. 50, 7939–7955.

Gupta, S.C., Larson, W.E., Linden, D.R., 1983. Tillage and surface residue effects on soil upper boundary temperatures. Soil Sci. Soc. Am. J. 47, 1212–1218.

He, Z.B., Zhao, W.Z., Liu, H., Chang, X.X., 2012. The response of soil moisture to rainfall event size in subalpine grassland and meadows in a semi-arid mountain range: a case study in northwestern China's Qilian Mountains. J. Hydrol. 420, 183–190.

Hiebert, E.N., 1963. Historical remarks on the discovery of argon: the first noble gas. In: Hyman, H.H. (Ed.), Noble-Gas Compounds. University of Chicago Press, Chicago, IL, pp. 3–20.

Intergovernmental Panel on Climate Change (IPCC), 2018. Special Report on Global Warming of 1.5 °C. . Available online at https://www.ipcc.ch/sr15/ (accessed January 04, 2019).

Jenkins, C., Cook, P.J., Ennis-King, J., Underschultz, J., Boreham, C., Dance, T., de Caritat, P., Etheridge, D.M., Freifeld, B.M., Hortle, A., Kirste, D., Paterson, L., Pevzner, R., Schacht, U., Sharma, S., Stalker, L., Urosevic, M., 2012. Safe storage and effective monitoring of CO_2 in depleted gas fields. Proc. Natl. Acad. Sci. USA 109 (2), 35–41.

Jenkins, C., Chadwick, A., Hovorka, S.D., 2015. The state of the art in monitoring and verification – ten years on. Int. J. Greenh. Gas Control 40, 312–349.

Johnson, G., Raistrick, M., Mayer, B., Shevalier, M., Taylor, S., Nightingale, M., Hutcheon, I., 2009. The use of stable isotope measurements for monitoring and verification of CO_2 storage. Energy Proc. 1, 2315–2322.

Kayler, Z.E., Sulzman, E.W., Rugh, W.D., Mix, A.C., Bond, B.J., 2010. Characterizing the impact of diffusive and advective soil gas transport on the measurement and interpretation of the isotopic signal of soil respiration. Soil Biol. Biochem. 42, 435–444.

Kharaka, Y.K., Cole, D.R., Hovorka, S.D., Gunter, W.D., Knauss, K.G., Freifeld, B.M., 2006. Gas–water–rock interactions in Frio Formation following CO_2 injection: implications for the storage of greenhouse gases in sedimentary basins. Geology 34, 577–580.

Kipfer, R., Aeschbach-Hertig, W., Peeters, F., Stute, M., 2002. Noble gases in lakes and ground waters. Rev. Miner. Geochem. 47 (1), 615–700.

Klusman, R.W., 2003. Rate measurements and detection of gas microseepage to the atmosphere from an enhanced oil recovery/sequestration project, Rangely, Colorado, USA. Appl. Geochem. 18, 1825–1838.

Klusman, R.W., 2006. Detailed compositional analysis of gas seepage at the National Carbon Storage Test Site, Teapot Dome, Wyoming, USA. Appl. Geochem. 21, 1498–1521.

Klusman, R.W., 2011. Comparison of surface and near-surface geochemical methods for detection of gas microseepage from carbon dioxide sequestration. Int. J. Greenh. Gas Control 5, 1369–1392.

Knapp, H.V., Angel, J.R., Atkins, J.R., Bard, L., Getahun, E., Hlinka, K.L., Keefer, L.L., Kelly, W.R., Roadcap, G.S., 2017. The 2012 Drought in Illinois. Report of Investigation 123. Illinois State Water Survey, Champaign.

Kuzyakov, Y., 2006. Sources of CO_2 efflux from soil and review of partitioning methods. Soil Biol. Biochem. 38, 425–448.

Larson, T.E., Breecker, D.O., 2014. Adsorption isotope effects for carbon dioxide from illite- and quartz-packed column experiments. Chem. Geol. 370, 58–68.

Leetaru, H.E., McBride, J.H., 2009. Reservoir uncertainty, Precambrian topography, and carbon sequestration in the Mt. Simon Sandstone, Illinois Basin. Environ. Geosci. 16, 235–243.

Leuning, R., Etheridge, D., Luhar, A., Dunse, B., 2008. Atmospheric monitoring and verification technologies for CO_2 geosequestration. Int. J. Greenh. Gas Control 2, 401–414.

Lewicki, J.L., Evans, W.C., Hilley, G.E., Sorey, M.L., Rogie, J.D., Brantley, S.L., 2003. Shallow soil CO_2 flow along the San Andreas and Calaveras Faults, California. J. Geophys. Res. Solid Earth 108, 2187. https://doi.org/10.1029/2002JB002141.

Lewicki, J.L., Hilley, G.E., Dobeck, L., Spangler, L., 2010. Dynamics of CO_2 fluxes and concentrations during a shallow subsurface CO_2 release. Environ. Earth Sci. 60, 285–297.

Liu, X.Z., Wan, S.Q., Su, B., Hui, D.F., Luo, Y.Q., 2002. Response of soil CO_2 efflux to water manipulation in a tallgrass prairie ecosystem. Plant Soil 240, 213–223.

Luo, Y., Zhou, X., 2006. Soil Respiration and the Environment. Elsevier Academic Press, Amsterdam, Netherlands.

Ma, J., Zheng, X.J., Li, Y., 2012. The response of CO_2 flux to rain pulses at a saline desert. Hydrol. Process 26, 4029–4037.

Mayer, B., Humez, P., Becker, V., Dalkhaa, C., Rock, L., Myrttinen, A., Barth, J.A.C., 2015. Assessing the usefulness of the isotopic composition of CO_2 for leakage monitoring at CO_2 storage sites: a review. Int. J. Greenh. Gas Control 37, 46–60.

Myers, M., Stalker, L., Pejcic, B., Ross, A., 2013. Tracers—past, present and future applications in CO_2 geosequestration. Appl. Geochem. 30, 125–135.

Myrttinen, A., Becker, V., van Geldern, R., Wurdemann, H., Morozova, D., Zimmer, M., Taubald, H., Blum, P., Barth, J.A.C., 2010. Carbon and oxygen isotope indications for CO_2 behaviour after injection: first results from the Ketzin site (Germany). Int. J. Greenh. Gas Control 4, 1000–1006.

Nickerson, N., Risk, D., 2013. Using subsurface CO_2 concentrations and isotopologues to identify CO_2 seepage from CCS/CO_2-EOR sites: a signal-to-noise based analysis. Int. J. Greenh. Gas Control 14, 239–246.

Palstra, S.W.L., Meijer, H.A.J., 2014. Biogenic carbon fraction of biogas and natural gas fuel mixtures determined with 14C. Radiocarbon 56, 7–28.

Qi, Y., Xu, M., Wu, J.G., 2002. Temperature sensitivity of soil respiration and its effects on ecosystem carbon budget: nonlinearity begets surprises. Ecol. Modell. 153, 131–142.

Riding, J.B., Rochelle, C.A., 2009. Subsurface characterization and geological monitoring of the CO_2 injection operation at Weyburn, Saskatchewan, Canada. In: Evans, D.J., Chadwick, R.A. (Eds.), Underground Gas Storage: Worldwide Experiences and Future Development in the UK and Europe. Geological Society of London, London, UK, pp. 227–256.

Risk, D., Kellman, L., Beltrami, H., 2002. Soil CO_2 production and surface flux at four climate observatories in eastern Canada. Glob. Biogeochem. Cycles 16, 69–71.

Romanak, K.D., Bennett, P.C., Yang, C., Hovorka, S.D., 2012. Process-based approach to CO_2 leakage detection by vadose zone gas monitoring at geologic CO_2 storage sites. Geophys. Res. Lett. 39. https://doi.org/10.1029/2012GL052426.

Romanak, K.D., Wolaver, B., Yang, C., Sherk, G.W., Dale, J., Dobeck, L.M., Spangler, L.H., 2014. Process-based soil gas leakage assessment at the Kerr Farm: comparison of results to leakage proxies at ZERT and Mt Etna. Int. J. Greenh. Gas Control 30, 42–57.

Schacht, U., Jenkins, C., 2014. Soil gas monitoring of the Otway Project demonstration site in SE Victoria, Australia. Int. J. Greenh. Gas Control 24, 14–29.

Schloemer, S., Furche, M., Dumke, I., Poggenburg, J., Bahr, A., Seeger, C., Vidal, A., Faber, E., 2013. A review of continuous soil gas monitoring related to CCS—technical advances and lessons learned. Appl. Geochem. 30, 148–160.

Schloemer, S., Moeller, I., Furche, M., 2014. Baseline soil gas measurements as part of a monitoring concept above a projected CO_2 injection formation—a case study from Northern Germany. Int. J. Greenh. Gas Control 20, 57–72.

Schoell, M., 1988. Multiple origins of methane in the earth. Chem. Geol. 71, 1–10.

Smith, K.A., Arah, J.R.M., 1991. Gas chromatographic analysis of the soil atmosphere. In: Smith, K. (Ed.), Soil Analysis. Marcel Dekker, New York, pp. 505–546.

Soil Survey Staff, 2014. Keys to Soil Taxonomy, 12th ed. U.S. Department of Agriculture, Natural Resources Conservation Service, Washington, DC.

Southon, J.R., 2007. Graphite reactor memory—where is it from and how to minimize it? Nucl. Instrum. Methods Phys. Res. B 259, 288–292.

Stuiver, M., Polach, H., 1977. Reporting of ^{14}C data. Radiocarbon 19, 355–363.

Trumbore, S.E., Davidson, E.A., Decamargo, P.B., Nepstad, D.C., Martinelli, L.A., 1995. Below ground cycling of carbon in forests and pastures of eastern Amazonia. Global Biogeochem. Cycles 9, 515–528.

Wang, H., Lundstrom, C.C., Zhang, Z., Grimley, D.A., Balsam, W.L., 2009. A mid-late Quaternary loess-paleosol record in Simmons Farm in southern Illinois, USA. Quat. Sci. Rev. 28, 93–106.

Whiticar, M.J., 1999. Carbon and hydrogen isotope systematics of bacterial formation and oxidation of methane. Chem. Geol. 161, 291–314.

Xu, L., Baldocchi, D.D., Tang, J., 2004. How soil moisture, rain pulses, and growth alter the response of ecosystem respiration to temperature. Glob. Biogeochem. Cycles 18. https://doi.org/10.1029/2004GB002281.

Xu, Q., Liu, S.R., Wan, X.C., Jiang, C.Q., Song, X.F., Wang, J.X., 2012. Effects of rainfall on soil moisture and water movement in a subalpine dark coniferous forest in southwestern China. Hydrol. Processes 26, 3800–3809.

Yang, C., Jamison, K., Xue, L., Dai, Z., Hovorka, S.D., Fredin, L., Treviño, H.R., 2017. Quantitative assessment of soil CO_2 concentration and stable carbon isotope for leakage detection at geological carbon sequestration sites. Greenh. Gases: Sci.

Technol. 7, 680–691.

Yener, D., Ozgener, O., Ozgener, L., 2017. Prediction of soil temperatures for shallow geothermal applications in Turkey. Renew. Sustain. Energy Rev. 70, 71–77.

Zhang, C.P., Gamage, R.P., Perera, M.S.A., Zhao, J., 2017. Characteristics of clay-abundant shale formations: use of CO_2 for production enhancement. Energies 10.